CONF-830406--38

DE83 012070

* Research sponsored by the Office of Fusion Energy, U.S. Department of Energy, under contract W-7405-eng-26 with the Union Carbide Corporation.

CONF-830406--38

NEUTRON ACTIVATION IN EBT-P

D. E. DRIEMEYER
McDonnell Douglas Astronautics Company-St. Louis Division
P. O. Box 516
St. Louis, Missouri 63166
(314) 576-8290

ABSTRACT

Neutron activation due to photoneutron production in the lead shields proposed to protect the EBT-P superconducting coils from excessive x-ray heating was investigated. The photoneutron flux distribution in various EBT-P structural components was calcualted for typical upgrade operating conditions using a standard two-dimensional transport model (TWOTRAN). Activity levels were then evaluated for major structural materials using activation cross sections tabulated in the GAMMON library. Activation dose rates in the device enclosure following several *days of 8h/day upgrade (90GHz)* operation were found to be ∿6 mrem/h, decaying to <0.25 mrem/h in ∿3 days. This requires radition monitoring of all personnel entering the device enclosure during this time, but should not generally restrict "hands on" access to the device. There is thus no strong motivation to replace lead with another shield material; however, it may be desirable to borate the enclosure walls in order to reduce the effect which impurities might have on activity levels.

INTRODUCTION

The high temperature (1-2 MeV) high beta (30%) electron rings that are needed for stability in an EBT plasma generate a large flux of hard x-rays. Lead shields are included in the EBT-P reference design [1] to protect the superconducting coils from excessive heating by these x-rays. Lead was selected over other candidate materials due to its low cost (it can be leased from the government whereas other materials would need to be purchased outright) and its shielding effectiveness. Unfortunately, lead has a low threshold energy for photoneutron production which may lead to activation problems during the proposed upgrade (90 GHz) phase of EBT-P operation. Problems are not expected during the initial (60 GHz) phase of operation because lower anticipated ring temperature and beta combine with the reduction in field strength to decrease photoneutron production by a factor of *∿100 relative to that at 90 GHz.*

The discussion presented here thus pertains to the following proposed mode of operation:

- Upgrade (90 GHz) configuration.
- 33% device availability (8 hours on 16 off continuously).
- 2 MeV ring electron temperature, relativistic Maxwellian tail.
- 30% ring beta.
- 2% aluminum impurity level in the plasma.
- Ring volume 10% of plasma volume.
- *Ring density 50% of the microwave cutoff* value.

These assumptions are intended to represent an attainable operating point, if EBT-P performs up to its expectations. It should be emphasized, however, that this operating point will certainly not be encountered until well into the upgrade phase of device operation. Furthermore, the assumption of a relativistic Maxwellian tail for the ring electron distribution results in a larger population of high energy electrons, hence hard x-rays, for a given ring temperature than is actually thought to exist based on EBT-S measurements. Present estimates of device activation can thus be regarded as conservative but are not worst case.

PHOTONEUTRON SOURCE EVALUATION

The spectrum of photon energies that is emitted from a typical EBT-P cavity for the operating conditions indicated above is illustrated in Figure 1. In this figure the direct component corresponds to Bremsstrahlumg emitted by ring electrons interacting with plasma ions, while the scattered component corresponds to Bremsstrahlumg emitted by ring electrons that strike the surface of the limiters. Of primary concern is the fraction of the distribution in excess of the 7 MeV threshold energy for photoneutron production in lead. This concern is underacored by the extensive view angle of the coil shields from the rings which exposes the

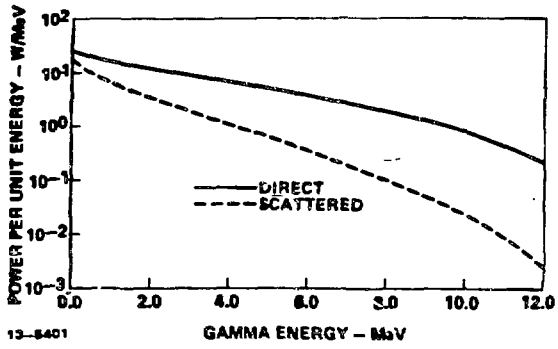

Figure 1. X-Ray Power Distribution for a Typical EBT-P Cavity Under Upgrade Operating Conditions.

lead to a large fraction of the emitted photons. Figure 1 shows that photons above 7 MeV come almost entirely from direct Bremsstrahlung. The present model thus assumes that all photons originate from the ring location as indicated in Figure 2.

The principal source of photoneutron cross sections comes from work done at Lawrence Livermore Laboratory [2, 3]. This work indicates that the photoneutron cross sections in lead are well approximated by a Lorentz-shaped resonance line

$$\sigma(E) = \sigma_o/(1 + (E_o^2-E^2)^2/E^2\Gamma^2) \qquad (1)$$

where values of the constants for the three lead isotopes are as follows:

	Pb-206	Pb-207	Pb-208
σ_o(mbarn)	514	481	639
E_o(MeV)	13.59	13.56	13.43
Γ(MeV)	3.85	3.96	4.07

Photons with energies above the 7 MeV threshold for photoneutron production are primarily forward scattering; hence the photon flux in these groups is almost directly proportional to the source strength. Equation 1 was thus averaged over the x-ray source distribution of Figure 1 to determine multigroup photoneutron cross sections which were inserted into the fission position of the appropriate gamma groups in the input cross section library. Fission fractions were evaluated by recognizing that photon absorption in lead results almost exclusively in neutron evaporation. The energy spectra of the evaporated neutrons is, therefore

$$f(E_n) = (E_n/T^2)\exp(-E_n/T) \qquad (2)$$

where E_n is the neutron energy and T the nuclear temperature which was set equal to 0.5 MeV.

In order to better represent the actual geometry of the photon source, lead coil shields and surrounding structure, a two-dimensional (r-z) radiation transport calculation was performed using the TWOTRAN code [4]. The actual calculational model is illustrated in Figure 2.

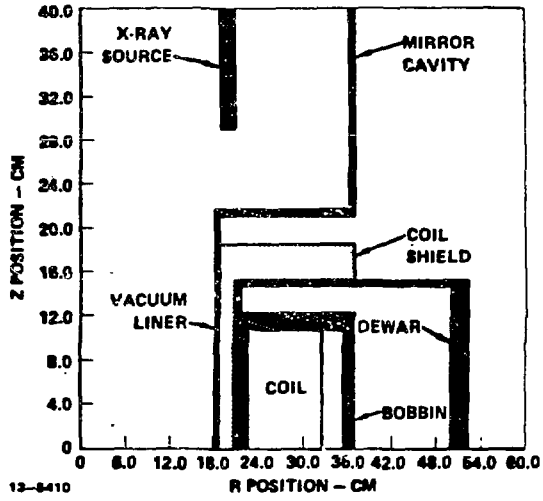

Figure 2. Spatial Configuration of the EBT-P Vacuum Vessel, Coil Shield, and Coil as Represented in the Twotran Model.

The EBT-P vacuum vessel was represented as an infinite bumpy cylinder where R = 0 corresponds to the axis of the cylinder or the center of the plasma, Z = 0 to a plane bisecting the coil, and Z = 40 cm to a plane mid-way between coils. The major structural boundaries are shown as they were defined in the model. Figure 2 thus encompasses the full extent in the axial direction since Z = 0 and Z = 40 cm are symmetry planes; however, in the radial direction the model extended out to R = 510 cm where the outer boundary of a 100 cm thick cylindrical concrete wall was located. The wall was included in order to pick up the backscatter contribution to the neutron flux within the device enclosure.

The transport calculations were carried out using an S-16 angular quadrature in order to minimize ray effects and a P-1 Legendre scattering expansion. The cross sections were taken from the 42 group (30 neutron/12 gamma) ENDFB/V library MATXS5, which is maintained on the NMFE computer network by MacFarlane, et. al., at Los Alamos National Laboratory. A 50/50 volume percent mix of water and stainless steel was used to represent the vacuum liner and mirror cavity, while 80% dense copper was used to represent the coil with pure theoretically dense lead used for the coil shield. The normal concrete composition was taken from Reference 5, and the coil bobbin and dewar were assumed to be pure stainless steel.

On the basis of the above model, the photoneutron production rate in the coil shields is found to be 2.2 x 10^{11} sec^{-1} for EBT-P upgrade operation. When distributed over the 36 coil shields, this source results in the neutron flux distribution shown in Figure 3. This figure illustrates the group summed photoneutron flux over the region encompassed by Figure 2, which has been superimposed over Figure 3 for clarity.

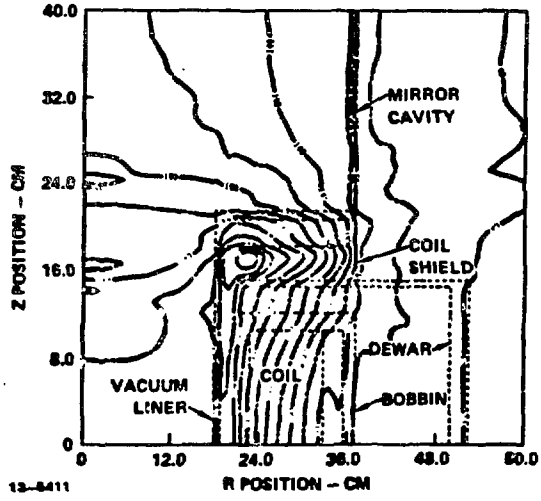

Figure 3. Photoneutron Flux Contours for 90GHz EBT-P Operation. Flux Units Have Been Multiplied by 10^{-4}, and the Structural Boundaries of Figure 2 Have Been Super-Imposed for Clarity.

As is expected the neutron flux peaks in the lead coil shield at a value of $\sim$4 x 10^6 n/cm^2/sec. The flux then falls rapidly to a value of $\sim$1 x 10^6 n/cm^2/sec while traversing the device structure after which it has attained a more or less uniform spatial distribution which is created primarily by backscatter from the walls. Because of the backscattered component, the flux thereafter decreases much more slowly falling only to $\sim$2 x 10^5 at the enclosure wall.

A key consideration in evaluating the activity produced by these neutrons is their energy distribution. Neutron energy spectra at three locations within the region defined by Figure 2 are shown in Figure 4 for a normal concrete enclosure. The three locations correspond to a point in the vacuum liner under the coil (18.5, 1.0), a point in the closeout of the coil dewar (52.0, 1.0), and a point in the mirror cavity (37.0, 39.0). The spectrum is quite similar at all three locations and is fairly well thermalized showing a local peak at low energies due to backscattering from the walls. As is expected, the thermal flux contribution is smallest under the coil where the backscattered

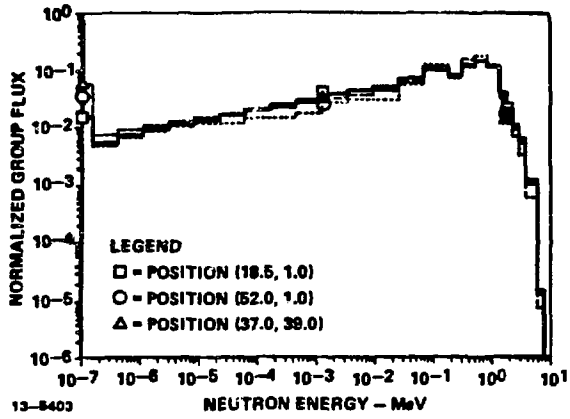

Figure 4. Neutron Energy Spectra at Three Locations Within the Device Structure with Normal Concrete Enclosure Walls. The Position Coordinates Are in Centimeters and, Referring to Figure 2, Correspond to Points in the Vacuum Liner, the Dewar, and the Mirror Cavity.

neutrons are most effectively shielded; however the variation in the overall flux spectrum over the device structure is seen to be minimal. One average flux spectrum can therefore be used to characterize the device components for the activation analyses.

The neutron flux energy distribution in EBT-P at points near and within the walls is much flatter at high energies and has a much larger thermal peak than those shown in Figure 4. The wall activity is therefore due almost entirely to (n, γ) interactions by the large thermal flux component, and this result is reflected in the wall-spectrum weighted activation cross sections discussed in the next section. Once again there is little variation in the energy spectrum over the wall structure, thus one average spectrum is used to characterize the wall flux for the activation analyses.

INDUCED ACTIVATION ANALYSES

General Discussion

The activity induced by neutron interaction in the EBT-P device enclosure is a complicated function of the constituent structural materials and configuration, the neutron flux spatial and energy distribution, and the device operation history. In adherence with the conservative philosophy of this analysis, the assumed operating history consists of a cyclic T hours on (24-T) off scenario. The activation buildup at the end of i successive periods of this cyclic operation, A_i, is

$$A_i = A_{i-1}e^{-24\lambda} + A_\infty(1-e^{-\lambda T}) \qquad (3)$$

where λ is the decay constant of the particular isotope of interest in inverse hours, A_{i-1} is the activity at the end of the previous operating period, and $A_\infty = n\sigma\phi$ is the activity that would build up if operation were continuous. In the expression for A_∞, n is the number of parent isotope atoms per gram of activated material, σ is the effective activation cross section and ϕ is the total neutron flux at the desired location. This equation shows that for continuous cycling the activity level saturates at a value, A_∞, found by equating A_{i-1} and A_i, namely

$$A_s = A_\infty\ (1 - e^{-\lambda T})\ /\ (1 - e^{-24\lambda}). \qquad (4)$$

For short half lives (< 3 h), this value is reached after one operating period and is more dependent on isolated operating time than on long term availability. Conversely for longer half lives (>> 1 day), the saturation level takes much longer to reach and is more dependent on overall availability than on isolated operating time. As a result, long term activation will be much less of a problem than short term because the experimental nature of EBT-P implies low overall availability.

The evaluation of specific activity levels for the major materials used in fabricating the EBT-P device was greatly simplified by drawing on the GAMMON library [6]. The GAMMON 100 x 25 group structure was collapsed into the LANL 30 x 12 group configuration used for the transport calculations and weighted by the neutron flux energy distribution expected at the vessel and wall to determine effective activation cross sections at these locations for the various isotopes contained in the library. This data was then used to selectively identify problem isotopes for which activity levels were calculated. The resulting activity levels were coupled with the gamma decay characteristics for each isotope to determine the gamma flux one meter from an isolated kilogram of the activated material. This gamma flux was converted to a dose rate using the flux-to-dose conversion factor of the American National Standard ANSI/ANS-6.1.1-1977. The result thus defines a biological dose rate experienced by an observer located one meter from a one kilogram point source of the activated material.

Summary of Activation Levels

The predominate materials found in the EBT-P device enclosure are stainless steel, copper, and concrete. Stainless steel forms the coil bobbin and dewar, the vacuum chamber, the device support structure, and most utility supply lines. Copper is the principal component of the coil pack itself, and concrete forms the device enclosure walls and roof. Table 1 summarizes these major component materials and their activity levels following an extended period of 8h/day device operation. The primary isotopes which contribute to the activity in each material are listed along with their decay half lives, effective activation cross sections, maximum activity per unit flux (A_∞/ϕ), cycling saturation fraction as defined by Equation 4, and the expected decay gamma dose rate per unit neutron flux per kilogram of activated material immediately following shutdown. It should be noted that the mass dependency has been eliminated from the dose rates presented for concrete isotope due to the planar nature of the

Table 1

Principal Isotopes Contributing to Initial Activation of Major EBT-P Component Materials

Parent Isotope	Atoms Per Gram Mat'l	Product Isotope	Half Life (ln2/λ)	$\langle\sigma_A\rangle$ (barns)	A_∞/ϕ (Ci-cm^{2}s/kg)	Saturation Fraction (A_s/A_∞)	Gamma Dose Rate Per Unit Flux (mrem-cm^{2}s/h-kg)
Mn-55	2.08+20*	Mn-56	2.6 h	9.69-1	5.45-12	0.883	4.32-9
Cr-50	8.99+19	Cr-51	27.7 d	1.08+0	2.62-12	0.336	1.89-11
Fe-58	2.13+19	Fe-59	44.6 d	9.12-2	5.25-14	0.335	1.37-11
Ni-58	9.04+20	Co-58	70.8 d	5.28-3	1.29-13	0.334	2.66-11
Mo-100	1.57+19	Mo-101	14.6 m	2.24-1	9.50-14	1.000	6.03-11
Stainless Steel Totals					8.35-12		4.44-9
Cu-63	6.55+21	Cu-64	12.7 h	3.07-1	5.43-11	0.485	4.69-9
Copper Totals					5.43-11		4.69-9
Na-23	4.35+20	Na-24	15.1 h	1.99-1	2.34-12	0.460	2.90-6
Al-27	9.91+20	Al-28	2.3 m	8.58-2	2.30-12	1.000	2.56-6
K-41	1.99+19	K-42	12.4 h	5.49-1	2.95-13	0.488	2.91-8
Concrete Totals					4.94-12		5.49-6**

* Note 2.08+20 denotes 2.08×10^{20}.

** Concrete values have units of (mrem-cm^{2}s/h). The mass dependency has been eliminated due to the planar nature of the source.

walls. This was accomplished by assuming that half of all decay gammas emitted within one mean free path of the surface make up the gamma flux emerging from the wall. For the present gamma spectrum one mean free path corresponds to ∿10cm.

An examination of Table 1 reveals some important characteristics of the material activation. Stainless steel activity is dominated by Mn-56 which has a 2.6h half life. The activity in all steel components will thus decrease by a factor of ∿500 during the first day after shutdown. During this same time, however, copper component activity levels, which are initially equivalent to those in steel, will only decrease by a factor of 4. Fortunately, the bulk of the copper in EBT-P is shielded by coil bobbins and dewars and should therefore contribute little to the overall activation dose rate within the device enclosure. The most important material from the standpoint of gaining uncontrolled access into the device enclosure is found to be concrete. Its initial activity level is lower than that in stainless steel, but the large exposed surface of concrete together with Na-24's 15.1h half life cause it to ultimately dominate the activation dose rate in the device enclosure, as will be seen in the next section.

Implications for Upgrade (90 GHz) Operation

The data summarized in Table 1 can in principal be combined with the neutron flux distribution to determine activation dose rates at various locations within the EBT-P device enclosure. This is in general a difficult procedure due to the complicated geometry of the structural components and resulting importance of self-shielding effects; however a rough estimate of the biological dose rate inside the enclosure can be obtained by considering a point located half way between the wall and the outer perimeter of the device immediately after shutdown. Based on the average neutron flux level in the first 10 cm of the wall (1.8×10^5 n/cm^{2}s) and the data in Table 1, the walls and floor will each contribute 1.0 mrem/h to the local dose rate at this point.

The dose contribution from the device structure at this point is more complicated. There are five major device components and they are summarized in Table 2 along with their single sector masses. This table also includes the average neutron flux over each of these components and the corresponding activation dose rate at one meter from the center of mass of the component assuming no self-shielding. The coil and vacuum liner masses are reasonably well shielded by the surrounding structure; therefore, their contribution to the dose rate can be neglected. As a result, the dose rate at one meter from a typical EBT-P sector is estimated to be 3.2 mrem/h immediately after shutdown, and since this dose is due almost entirely to the Mn-56 component, it will decay with a 2.6 hour half life. Five sectors contribute most of the dose at a point mid-way between the device perimeter and the wall, and the center of mass of all of these sectors is further than one meter from the point of interest. The dose rate due to device structural activity is therefore ∿4.3 mrem/h, and this combines with the wall and floor contribution to produce a total dose rate of ∿6.3 mrem/h at the mid-way point between device and the wall.

Table 2

Summary of Device Component Masses and Activities

Component	Material	Mass (kg)	Average Neutron Flux (n/cm^{2}s)	One Meter Dose Rate (mrem/h)
Coil	Copper	228	1.8E6	1.9
Bobbin	Steel	173	2.4E6	1.1
Dewar	Steel	345	5.0E5	0.8
Vacuum Liner	Steel	75	2.1E6	0.7
Mirror Cavity	Steel	282	1.0E6	1.3

This result is significant in that it is above the free access limit and will therefore require radiation monitoring of personnel entering the device enclosure, but it is certainly not large enough to cause a great deal of concern. This is especitally true when coupled with the fact that it is composed primarily of Mn-56 and Na-24 which have half lives of 2.6 and 15.1 hours respectively. After one day the dose rate will be due almost entirely to the wall component (Na-24) which requires 3 days to fall below the free access limit. The device enclosure will thus need to be a controlled access area for approximately 3 days after shutdown with normal concrete walls; however, the dose rates are quite low and therefore should not impose any significant hazard to personnel. In fact, if an individual entered the enclosure immediately after shutdown and stayed indefinitely he would receive less than the allowable weekly dose for workers in a radiation area of 100 mrem.

SUMMARY AND CONCLUSIONS

Neutron activation levels in EBT-P have been investigated and found to be slightly in excess of free access limits following upgrade operation with both normal concrete and borated concrete walls. The total activation dose rate immediately after shutdown is projected to be ∿6.3 mrem/h for normal concrete, and it is due primarily to Mn-56 in the stainless steel which has a 2.6 hour half life and Na-24 in the concrete which decays with a 15.1 hour half life. The Mn-56 component initially exceeds the contribution

from Na-24 by a factor of 2; however, after one day the Na-24 component dominates due to its longer half life. As a result, access into a normal concrete device enclosure will need to be controlled for approximately three days after shutdown. This is illustrated by the upper curve in Figure 5 which shows the decay in residual EBT-P activity following an extended period of 8 hour on/16 hour off 90 GHz operation.

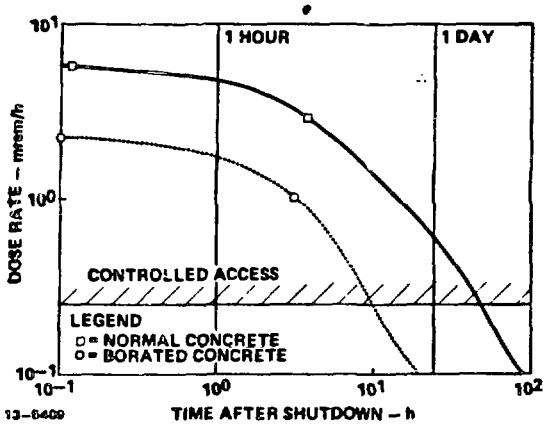

Figure 5. Decay of Residual Neutron-Induced Activity in EBT-P After Shutdown Following an Extended Period of 8-Hour On/16-Hour Off Operation. Both Curves Are Calculated for a Point Midway Between the Torus and the Wall as Discussed in the Text.

Figure 5 also shows the reduction in residual EBT-P activity resulting from adding 0.5% boron by weight to the concrete used to construct the device enclosure. This decreases the thermal neutron flux in the device structure and consequently reduces device activity by roughly a factor of two. A more important effect of the boron, however, is a factor of 20 reduction in wall activity as compared to the normal concrete case. This causes the wall dose component to be less than the free access limit at all times after shutdown; thus shortening the controlled access period from ∿3 days to ∿10 hours, as indicated on Figure 5. In addition, the lower thermal neutron flux in the wall also reduces the chance of concrete impurities with large neutron capture cross sections contributing significantly to activation levels in the device enclosure. These benefits must, of course, be weighed against the increased cost of the borated concrete before a final judgement can be made.

In conclusion it appears that the use of lead for shielding the coils from excess x-ray heating poses no significant biological hazards. Following 90 GHz operation, access into the device enclosure will need to be controlled for a few days, but dose rates are low enough that personnel residency should not be restricted due to radiation exposure. Due to the "order of magnitude" nature of this study, however, it is recommended that data acquired during the baseline phase of operation be used to verify and update the assumptions which were made in evaluating the present x-ray emission spectra. This is particularly important because a change in the assumed shape and cutoff of the ring electron energy distribution tail can significantly alter photoneutron production rates and the resulting activity levels.

REFERENCES

1. Elmo Bumpy Torus Proof of Principle Phase II-Title 1 Report, Vol. III, McDonnell Douglas Astronautics Company Report EBT-P010 (1982).

2. B. L. Berman (comp.), "Atlas of Photoneutron Cross Sections Obtained With Monoenergetic Photons," Lawrence Livermore National Laboratory Report, UCRL-75694 (1974).

3. B. L. Berman (comp.), "Atlas of Photoneutron Cross Sections Obtained With Monoenergetic Photons," Lawrence Livermore National Laboratory Report, UCRL-78482 (1976).

4. K. D. Lanthrop and F. W. Brinkley, "TWOTRAN-II: An Interfaced Exportable Version of the TWOTRAN Code for Two-Dimensional Transport," Los Alamos National Laboratory Report, LA-4848-MS (1973).

5. R. G. Jaegar (ed.), Engineering Compendium on Radiation Shielding, Vol. II (Springer-Verlag Berlin/Heidelberg, 1975).

6. M. E. Battat, R. J. LaBauve, D. W. Muir, "The GAMMON Activation Library," Los Alamos National Laboratory Report, LA-8040-MS (1979).

This work was performed under subcontract 22X-21099C to Union Carbide Corporation under contract W-7405-eng-26 with the Office of Fusion Energy, U.S. Department of Energy.

DISCLAIMER